

Gaps and Challenges in Microdosimetry: Improvements With Realistic Models of Endoplasmic Reticulum

A. De Angelis, L. Caramazza, F. M. Andre, C. Merla, L. M. Mir, F. Apollonio, and M. Liberti

Abstract – In bioelectromagnetics it can be crucial to estimate electric quantities at the microscopic scale, to establish a connection between the external applied field and the observed effects. Here we present a microdosimetric study based on a 2D realistic model of a cell and its endoplasmic reticulum. The analysis is quantified in terms of electric field and transmembrane potential induced by an external applied 10 ns pulsed electric field. This study opens the way to numerically assisted experiments for control and biomanipulation of cells and subcellular organelles.

1. Introduction

Microdosimetry is required for evaluating the spatial, temporal, and spectral distributions of electromagnetic (EM) fields imparted to cellular and subcellular structures, such as cell membranes and organelles [1]. Recently, several works addressing this issue have been published [2, 3], and a great interest has come also from the key role that microdosimetry plays in estimating the transmembrane potential (TMP) induced by the pulsed electric field in the electroporation of cells and tissues [4–7].

A microdosimetric study requires two basic steps: the setup of a suitable dielectric and geometrical model and the choice of an appropriate EM solution. The most common choice for the model is the three-layered cell [1–8], which includes cytoplasm, a plasma membrane, and an extracellular medium. Some models consider simplified intracellular compartments such as the endoplasmic reticulum, nucleus, or bound water layers [9–11]. Concerning the choice of appropriate EM solution, the most popular one is a quasi-static approach. Indeed, at the single-cell level, even in the

microwave range, the involved wavelength is much greater than the cell size (millimeter versus micrometer). To consider the frequency dependence of the induced field, the complex permittivity of the cellular compartments is used in the models.

Microdosimetric analyses are very useful in dealing with ultrashort pulsed electric fields (of microsecond and nanosecond duration), that are able to effectively electroporabilize the cell membranes when overcoming a given induced TMP threshold [12]. Nanosecond pulses, with amplitudes of the order of megavolts per meter, due to their higher frequency content, permeabilize the subcellular membranes (endoplasmic reticulum [ER] membranes) [13]. The ER is a large, dynamic structure that serves many roles in the cell, including calcium storage, protein synthesis, and lipid metabolism [14]. Hence, in recent years microdosimetric models including compartments like the ER have attracted increasing interest.

In this article, we present a 2D realistic model of a single cell and its ER. Microdosimetric analysis of the electric fields, the TMP induced by the pulsed electric field, and membrane pore densities occurring at the levels of plasma and ER membranes are presented when the sample is exposed to a pulsed electric field of 10 ns.

2. Modeling Realistically Shaped Cell Organelles

To obtain a 2D microdosimetric model representative of the real biological target, images obtained by confocal microscopy using staining techniques were used to identify different cell regions, following the techniques described in [15, 16]. Realistic cell models were imported into COMSOL and electric properties as in [16] were assigned to the different compartments. The 10 ns pulsed electric field was varied from 4 MV/m to 8 MV/m. The steady-state problem has been solved in the Electric Currents mode considering: 1) the Electric Currents application mode of the AC/DC module (time-dependent study); and 2) the boundary ordinary differential equations and differential-algebraic equations application of the Mathematics module. For all boundaries, continuity conditions were set. Moreover, the Contact Impedance condition was imposed on the cell and ER membranes. The pore formation dynamics were studied through the asymptotic model proposed by DeBruin and Krassowska [17], using the same formulas and parameter values reported in [16]. Membrane conductivity in electroporation conditions is calculated as the sum of the equilibrium

Manuscript received 1 February 2022..

A. De Angelis, L. Caramazza, F. Apollonio and M. Liberti are with Center for Life Nano- & Neuro-Science, Fondazione Istituto Italiano di Tecnologia (IIT), Rome, 00161, Italy. e-mail: annalisa.deangelis@iit.it

L. Caramazza, F. Apollonio and M. Liberti are with Department of Information Engineering, Electronics and Telecommunications, Sapienza University of Rome, Rome, Italy. email: laura.caramazza@uniroma1.it, francesca.apollonio@uniroma1.it, micaela.liberti@uniroma1.it

F.M. Andre and L.M. Mir are with UMR 9018 METSY, CNRS, Université Paris-Saclay, Gustave Roussy, Villejuif 94805, France. email: Franck.ANDRE@cnrs.fr, luis.mir@cnrs.fr

C. Merla is with Italian National Agency for Energy New Technologies and Sustainable Economic Development (ENEA), Division of Health Protection Technologies, Via Anguillarese 301, Rome, 00123, Italy. email: caterina.merla@enea.it

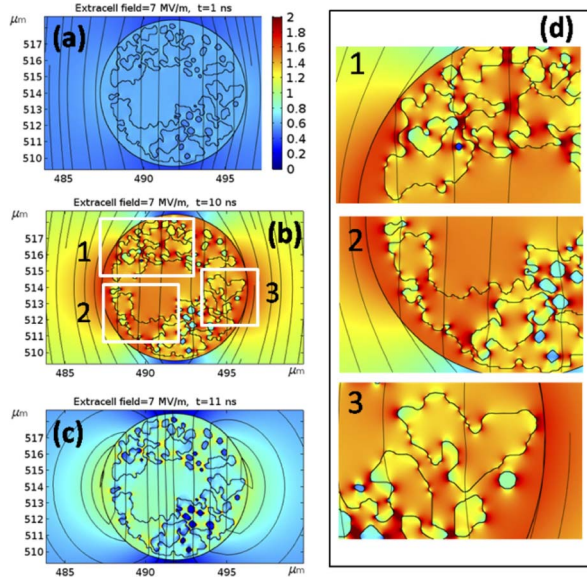


Figure 1. Electric field distribution and current density streamlines at (a) 1 ns (half rise time), (b) 10 ns (the end of the pulse plateau), and (c) 11 ns (half fall time) on the cell and ER for an external field of 7 MV/m. The legends on the graph are reported in megavolts per meter. Zoomed areas corresponding to the selected windows (1, 2, and 3 in b) are shown in (d).

membrane conductivity and the conductivity changes due to the formation of pores in the membrane, as in [18].

3. Results

A systematic analysis of the effects induced on the plasma and the ER membranes was performed through a time-domain study implemented for a trapezoidal 10 ns electric pulse (2 ns rise and fall times). Four different pulse amplitudes were simulated—4 MV/m, 6 MV/m, 7 MV/m, and 8 MV/m—to identify the field intensity necessary for poration onset of the membranes of the biological system “cell with ER”.

The electric field distributions and the current densities around the cell and in the ER were normalized to the amplitude of the extracellular field (7 MV/m). These data are shown for three time instants of the applied pulse (1 ns, 10 ns, and 11 ns; left column of Figure 1) and three different regions of the domain of interest (right column of Figure 1). At $t = 10$ ns, when the electric pulse is at the end of its plateau (Figure 1b), the plasma membrane is porated, and consequently the electric field within the cell is higher, probably due to the pore conduction that becomes more important than passive displacement currents [19].

Moreover, as the irregular shape of the ER membrane causes changes in the intensity and directions of the electric field, the intracellular electric field is distributed nonuniformly, as better evident in the zoomed regions 1, 2, and 3 of Figure 1d. At half of the fall time ($t = 11$ ns, Figure 1c), the internal electric field

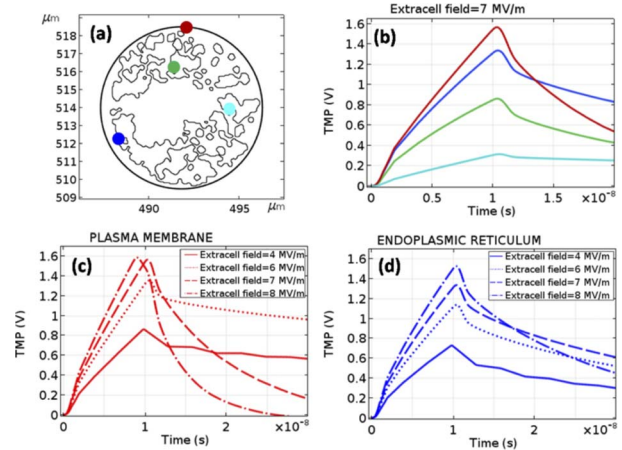


Figure 2. Induced TMP as a function of time for (a) the four selected points for (b) a selected applied pulse amplitude of 7 MV/m and (c) for the red point on the plasma membrane and (d) the blue point on the ER for different external pulse amplitudes (4 MV/m, 6 MV/m, 7 MV/m, 8 MV/m).

decreases following the external one, but in those regions where the induced electroporation was extensive, a higher electric field is sustained for some time after the pulse end. To perform a more quantitative evaluation of the phenomenon, the TMP induced by the applied electric field was considered; the TMP is equal to the line integral across the membrane thickness d of the electric field induced in the membrane itself ($\text{TMP} = \int_d \vec{E} \cdot d\vec{l}$), and it represents a valid indicator of the occurrence of electroporation. Indeed, when the TMP passes a specific threshold, pore creation starts. Experimental studies report different electroporation thresholds, ranging from 0.2 V to 1 V depending on cell type and experimental conditions [13]. Figure 2b shows the TMP evaluated at different selected points (small circles in Figure 2a). The TMP of the plasma membrane is chosen at the red circle, and that of the ER at the blue, cyan, and green circles in Figure 2a. The TMP for the ER ranges from 20% to 80% of that of the plasma membrane, depending on the chosen position. This suggests that a 10 ns pulsed electric field is potentially able to partially porate the ER with electric field values slightly greater than the ones needed to porate the plasma membrane. This result is clearly related to the frequency content of the pulsed electric field (up to 100 MHz) that can partially shortcut the plasma membrane.

Consequently, nanosecond pulses can penetrate the cell and induce a remarkable TMP value for the ER membrane, with differences related to the irregular shape of the organelle and the selected points. The TMP induced by the four selected extracellular fields (4 MV/m, 6 MV/m, 7 MV/m, 8 MV/m) at the plasma membrane (red point) and the blue point at the ER membrane are reported in Figure 2c and 2d, respectively. These results show that an extracellular field of 4 MV/m is not sufficient to induce a $\text{TMP} \geq 1$ V, chosen here as permeabilization threshold. The region of

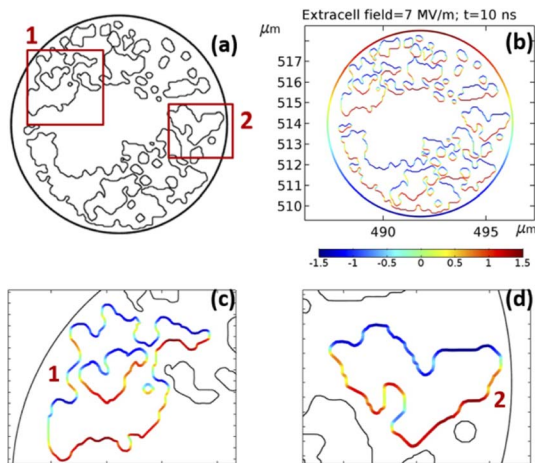


Figure 3. (a) Induced TMP spatial distribution at 10 ns for an applied pulse amplitude of 7 MV/m. The legends of the graphs are reported in volts. (b) TMP distribution on the entire investigated domain. (c, d) Zoomed areas of ER corresponding to the red windows in (a).

the plasma and ER membranes identified by the selected points reaches 1 V already at 6 MV/m, whereas other regions of the ER membrane show a different behavior, with a TMP estimated at those points < 1 V also for an applied field of 7 MV/m (Figure 2b).

This trend is confirmed by the TMP along all the boundaries of the domain of interest at the end of the pulse plateau ($t = 10$ ns), reported in Figure 3. For an amplitude of 7 MV/m, the plasma membrane reached the same TMP value at the anodic and cathodic poles with inverted polarity. The plasma transmembrane voltage increases to approximately 1.5 V in 10 ns before the onset of reversible electrical breakdown, representing an evident signature of electroporation [20, 21]. It is interesting to note that ER membranes behave nearly identically to the plasma membrane in their response, with an inverted polarity, as expected (Figure 3b). As is better visible in the zoomed regions 1 and 2 in Figure 3, the TMP of the ER membrane has different values depending on the position of the observation points. The extremely folded ER membrane experiences different TMP, since the cosine law in Schwan's equation [8] loses its validity in irregular structures, as reported in [13, 22].

4. Conclusions

The aim of this work was to consider irregularly shaped cells and organelles and perform a systematic analysis for an applied external field lasting 10 ns. Some results have been presented stressing the importance of realistic ER modeling in a 2D model. An important point addressed in this article is the possibility of relating electroporation phenomena occurring at the cellular level to those on a subcellular scale via a fast but reliable and realistic model, opening the way to numerically assisted experiments for control and biomanipulation of cells and subcellular organelles.

5. References

1. F. Apollonio, M. Liberti, A. Paffi, C. Merla, P. Marracino, et al., "Feasibility for Microwaves Energy to Affect Biological Systems via Nonthermal Mechanisms: A Systematic Approach," *IEEE Transactions on Microwave Theory and Technique*, **61**, 5, May 2013, pp. 2031-2045.
2. T. Kotnik and D. Miklavčič, "Theoretical Evaluation of the Distributed Power Dissipation in Biological Cells Exposed to Electric Fields," *Bioelectromagnetics*, **21**, 5, July 2000, pp. 385-394.
3. M. Liberti, F. Apollonio, C. Merla, and G. d'Inzeo, "Microdosimetry in the Microwave Range: A Quantitative Assessment at Single Cell Level," *IEEE Antennas Wireless Propagation Letters*, **8**, July 2009, pp. 865-868.
4. K. C. Smith, T. R. Gowrishankar, A. T. Esser, D. A. Stewart, and J. C. Weaver, "The Spatially Distributed Dynamic Transmembrane Voltage of Cells and Organelles Due to 10 ns Pulses: Meshed Transport Networks," *IEEE Transactions on Plasma Science*, **34**, 4, August 2006, pp. 1394-1404.
5. C. Merla, A. Paffi, F. Apollonio, P. Leveque, G. d'Inzeo, et al., "Microdosimetry for Nanosecond Pulsed Electric Field Applications: A Parametric Study for a Single Cell," *IEEE Transactions on Biomedical Engineering*, **58**, 5, May 2011, pp. 1294-1302.
6. C. Merla, A. Denzi, A. Paffi, M. Casciola, G. d'Inzeo et al., "Novel Passive Element Circuits for Microdosimetry of Nanosecond Pulsed Electric Fields," *IEEE Transactions on Biomedical Engineering*, **59**, 8, August 2012, pp. 2302-2311.
7. S. Muñoz, J. L. Sebastián, M. Sancho, and J. M. Miranda, "Transmembrane Voltage Induced on Altered Erythrocyte Shapes Exposed to RF Fields," *Bioelectromagnetics*, **25**, 8, December 2004, pp. 631-633.
8. K. R. Foster and H. P. Schwan, "Dielectric Permittivity and Electrical Conductivity of Biological Materials," Part I, pages 27-98, in *CRC Handbook of Biological Effects of Electromagnetic Fields*, C. Polk and E. Postw, Eds., 1st Ed., Boca Raton, FL, CRC Press, 1986.
9. A. Denzi, C. Merla, P. Camilleri, A. Paffi, G. d'Inzeo, et al., "Microdosimetric Study for Nanosecond Pulsed Electric Fields on a Cell Circuit Model With Nucleus," *The Journal of Membrane Biology*, **246**, no. 10, October 2013, pp. 761-767.
10. M. Simeonova and J. Gimsa, "The Influence of the Molecular Structure of Lipid Membranes on the Electric Field Distribution and Energy Absorption," *Bioelectromagnetics*, **27**, 8, December 2006, pp. 652-666.
11. T. Kotnik and D. Miklavčič, "Second-Order Model of Membrane Electric Field Induced by Alternating External Electric Fields," *IEEE Transactions on Biomedical Engineering*, **47**, 8, August 2000, pp. 1074-1081.
12. M. Breton and L. M. Mir, "Microsecond and Nanosecond Electric Pulses in Cancer Treatments," *Bioelectromagnetics*, **33**, 2, February 2012, pp. 106-123.
13. M. A. De Menorval, F. M. Andre, A. Silve, C. Dalmay, O. Français, et al., "Electric Pulses: A Flexible Tool to Manipulate Cytosolic Calcium Concentrations and Generate Spontaneous-Like Calcium Oscillations in Mesenchymal Stem Cells," *Scientific Reports*, **6**, August 2016, p. 32331.
14. D. S. Schwarz and M. D. Blower, "The Endoplasmic Reticulum: Structure, Function and Response to Cellular Signaling," *Cellular and Molecular Life Sciences*, **73**, January 2016, pp. 79-94.
15. A. Denzi, F. Camera, C. Merla, B. Benassi, C. Consales, et al., "A Microdosimetric Study of Electropulsation on

- Multiple Realistically Shaped Cells: Effect of Neighbours,” *Journal of Membrane Biology*, **249**, October 2016, pp. 691-701.
16. A. De Angelis, A. Denzi, C. Merla, F. M. Andre, L. M. Mir, et al., “Confocal Microscopy Improves 3D Microdosimetry Applied to Nanoporation Experiments Targeting Endoplasmic Reticulum,” *Frontiers in Bioengineering and Biotechnology*, **8**, September 2020, p. 552261.
 17. K. A. DeBruin and W. Krassowska, “Modeling Electroporation in a Single Cell. I. Effects of Field Strength and Rest Potential,” *Biophysical Journal*, **77**, 3, September 1999, pp. 1213-1224.
 18. B. Mercadal, P. T. Vernier, and A. Ivorra, “Dependence of Electroporation Detection Threshold on Cell Radius: An Explanation to Observations Non Compatible With Schwan’s Equation Model,” *The Journal of Membrane Biology*, **249**, October 2016, pp. 663-676.
 19. T. R. Gowrishankar, A. T. Esser, Z. Vasilkoski, K. C. Smith, and J. C. Weaver, “Microdosimetry for Conventional and Supra-Electroporation in Cells With Organelles,” *Biochemical and Biophysical Research Communications*, **341**, 4, March 2006, pp. 1266-1276.
 20. D. A. Stewart Jr., T. R. Gowrishankar, and J. C. Weaver, “Transport Lattice Approach to Describing Cell Electroporation: Use of a Local Asymptotic Model,” *IEEE Transactions on Plasma Science*, **32**, 4, August 2004, pp. 1696-1708.
 21. S. A. Freeman, M. A. Wang, and J. C. Weaver, “Theory of Electroporation of Planar Bilayer Membranes: Predictions of the Aqueous Area, Change in Capacitance, and Pore-Pore Separation,” *Biophysical Journal*, **67**, 1, July 1994, pp. 42-56.
 22. H. Hanna, A. Denzi, M. Liberti, F. M. André, and L. M. Mir, “Electropermeabilization of Inner and Outer Cell Membranes With Microsecond Pulsed Electric Fields: Quantitative Study With Calcium Ions,” *Scientific Reports*, **7**, October 2017, p. 13079.